Available online at www.sciencedirect.com
SCIENCE DIRECT®
Physica B 363 (2005) 1–6
PHYSICA B
www.elsevier.com/locate/physb

Preparation of InP–SiO_2 3D photonic crystals

Tan Chunhua*, Fan Guanghan, Zhou Tianming, Li Shuti, Sun Huiqing

Institute of Opto-electronic Materials and Technology, South China Normal University, Zhongshan Street, Guangzhou 510631, People's Republic of China

Received 11 July 2004; received in revised form 12 January 2005; accepted 13 January 2005

Abstract

Fabricated artificial opal templates and low pressure metal-organic chemical-vapor deposition have been used to infill the voids within opals and optimized the growth parameters. Scanning electron microscopy images, X-ray diffraction and reflection spectra results show that the InP is homogeneously distributed inside the opals, with high crystalline quality. The filling ratios of InP in the voids is about 12.8% and the photonic band gap is shifted to higher wavelength as a result of the high contrast of dielectric constants when InP is introduced which are in agreement with theoretical calculations.

PACS: 81.15.Gh; 78.65.Jd; 77.90.+k

Keywords: Artificial opals; Photonic band gap; Photonic crystal; Metal-organic chemical-vapor deposition; Scanning electron microscopy; Spectacular reflectivity

1. Introduction

Photonic crystal (PC) is the name given to a structure that possesses periodic dielectric constant with a length scale of the same order as the wavelength of the electromagnetic radiation. Because photonic crystals can control the flow of photons, it has many applications in low-loss wave guides, optical cavities, zero threshold microlasers, light-emitting diodes, optical switches and tunable filters. Since Yablonovich [1] suggested the idea of photonic bands, there has been an increasing interest in studying the photonic band gap (PBG) structures in one-, two-, and three-dimensional (1D, 2D, 3D) systems. Now, it has achieved great success in fabricating 1D and 2D PCs. However, the realization of photonic crystals for optical or near infrared (IR) frequencies is still a major technological challenge.

Synthetic opals made by means of sedimentation and ordering of SiO_2 nanospheres have been shown to be excellent candidates to build up 3D

*Corresponding author. Tel.: 86 02085211435; fax: 86 02085210809.
E-mail address: tch2000@163.com (T. Chunhua).

0921-4526/$ - see front matter © 2005 Elsevier B.V. All rights reserved.
doi:10.1016/j.physb.2005.01.399

PCs in the near-infrared-visible range [2–8]. Opals have been proven to form a FCC lattice and demonstrated a pronounced stop band in transmission and reflectance spectrum [9]. However, the resultant refractive index contrast between silica and air (1.5:1) is weak, natural and artificial opal do not exhibit a complete photonic gap, since its stop bands for different in the Brillouin zone do not overlap. Infilling the air voids within opals with higher index semiconductor can suppress the density of photonic states and improve the photonic properties, even to produce a full PBG material. Some work on semiconductor infilled opals has been reported [10–14].

In this paper, we present an experimental procedure designed to grow high-quality InP in the opal voids, using metal-organic chemical-vapor deposition (MOCVD). The homogeneous distribution of the high ε ($\varepsilon = 12.7$) guest material in the low ε host achieved by this method gives rise to enhanced photonic crystal properties as has been proved by enhanced photonic reflectance measurements. The aim of this work is to provide a foundation for fabricating 3D PCs devices.

2. Experimental

The monodispersed ($<5\%$) opal spheres were fabricated following the Stober–Fink–Bohn process. The hydrolysis of tetraethoxysilane (TEOS) and later polymerization of Si–O chains in an ethanol medium with ammonium hydroxide as a catalyst is used, with sphere sizes varying from 200 to 600 nm by controlling the hydrolysis conditions. There are a few methods to assemble order colloidal crystal from monodispersed opal spheres, such as natural sedimentation [15], electrophoresis [16], centrifugation [7], solvent vaporization, etc. For the need to infill InP by MOCVD, we assembled the opal photonic crystal templates in an FCC arrangement on GaAs substrate (15° off the (1 0 0) plane towards the (0 1 1) direction) by means of solvent vaporization. The steps involved are: make opal spheres to be colloidal suspension in ethanol, then dip the GaAs substrate into suspension about 10 h, after ethanol is vaporized, the suspensions are dried to form a film. The samples present opalescence colors, which come from the Bragg diffraction effects of the ordered silica solid dielectric structure.

Before the opal photonic crystals are filled with a precursor, it is desirable to sinter them. The sintering process strengthens the opals and forms the necks to connect every sphere with its neighbors; the sintering process also permits to control the opal void volume for subsequent semiconductor infilling, and induces connected network topology, allowing the removal of the template by acid etching. The sintering took place at 650 °C for 3 h in N_2 ambient.

The InP was grown in the opal by the use of a low pressure-MOCVD (LP-MOCVD) in a horizontal reactor of the EMCORE (GS/3200) at a pressure of 60 torr and a growth temperature of 550 °C. Palladium-purified hydrogen was used as the carrier gas, trimethylindium (TMIn) was used as the group III source, and phosphine was used as the group V reactants.

Prior to growth, the samples were heated to temperatures of up to 700 °C in the reactor under a flow of H_2 gas to remove moisture, grease and besmirch, followed by a nucleating process that the sources are decomposed to nucleate in a low temperature (380 °C) and low flux of sources. Because it is believed that deposition begins with nucleation at defects on the surface of silica balls before nucleus grows. The growth temperature is lower than that normally employed in InP MOCVD, which is due to the catalytic nature of the silica surface exposed to TMIn, and this surface-driven reactions often result in growth at temperatures considerably lower than those used in conventional MOCVD. Low-pressure is necessary to drive sources diffusion into the voids, and accordingly improve the infilling ratio of the InP. During the growth process, phosphine (450 ccm) was passed through the reactor without interrupt, however TMIn (180 ccm) was passed for 1 min then interrupted for 3 min, and each cycle was for 4 min. With the above cycle being repeated 20 times, higher loading of InP can be achieved.

After InP growth, the samples were heated to 690 °C in order to improve the semiconductor crystallization and to allow diffusion of InP inside

the void structure. The experiments were carried out to arrange different opal samples.

3. Characterization

Scanning electron microscopy (SEM) micrographs were taken to study the morphology and distribution of the InP grown inside the opals using a Philips XL-30-ESEM-FEG instrument operating at 15.0 or 20.0 kV. Fig. 1 corresponds to an internal (1 1 1) family surfaces of opals (sphere size $d = 250$ nm) without infilling InP. Figs. 2 and 3 show the details of the surface and cleaved edge of a sample infilled with InP. In this sample, InP crystals can be clearly seen on the sphere surfaces, distinguished from the sphere surfaces of the bare opal (Fig. 1). The SEM images show that the InP is not only covering the sphere surfaces but also infilling the interstitials between the silica spheres. The phases in the sample were detected by a D/max-3C X-ray diffraction meter (XRD) with Ni-filtered Cu $K\alpha$ radiation ($U = 40$ kV, I = 100 mA) at a scanning rate of 4°/min. Fig. 4 is the XRD spectra of

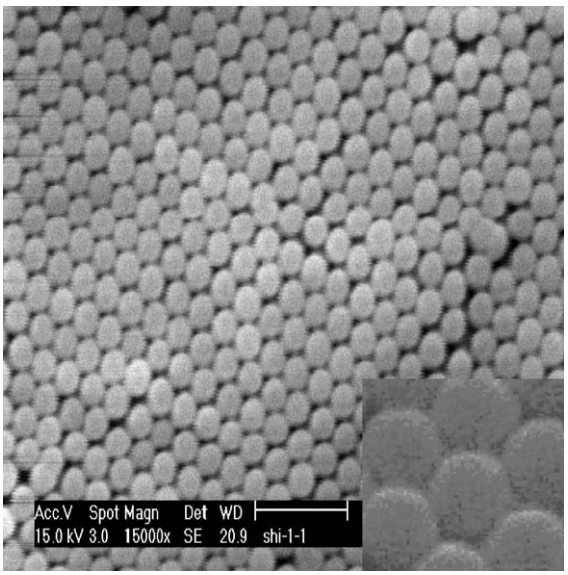

Fig. 1. SEM image of internal (1 1 1) facet of a bare opal. Inset is the enlarged image of the same sample.

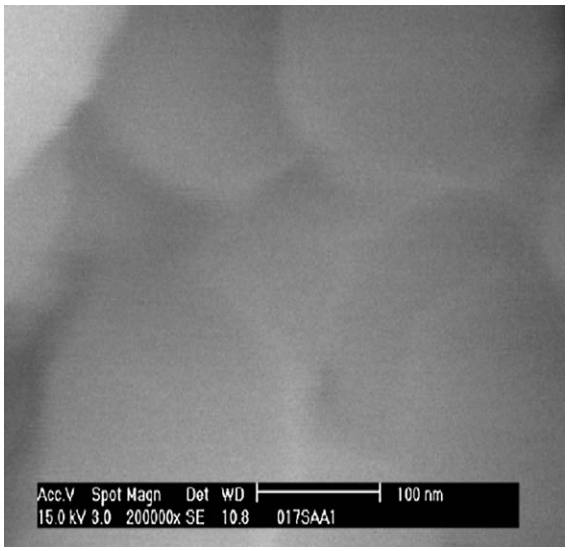

Fig. 2. SEM image of a 0.5 μm × 0.5 μm area of infiltrated opal surface.

InP–SiO_2 photonic crystals, which is in agreement with the standard spectrum of InP, showing that InP is of good quality and the distribution is very homogeneous in the matrix. From the SEM images, it can be seen that the InP surface is smooth, indicating that the growth of the InP-wetting layer is independent of the local characteristics of the opal template. Maybe owing to the fact that the procedure employed in this work is more closely related to that employed under atomic layer epitaxy conditions. As a consequence, the 3D periodicity of the template is inherited by the guest material, which is in good agreement with the opal-InP composites optical feature.

The most direct way to measure the photonic stop band behaviors is by optical reflectance. Photonic crystal optical properties of bare and InP infilled crystals were proved by means of specular reflectance measurements in a UV-2550 UV–VIS–NIR spectrophotometer using plane white light from a tungsten, holographic grating as the spectroscope with a resolution of 0.2 nm, the slit width is 2.0 nm and a photomultiplier tube as the detector was used, the diameter of the detecting spot is 2 mm. Fig. 5 shows specular reflectance spectra from the (1 1 1) surface at 90°

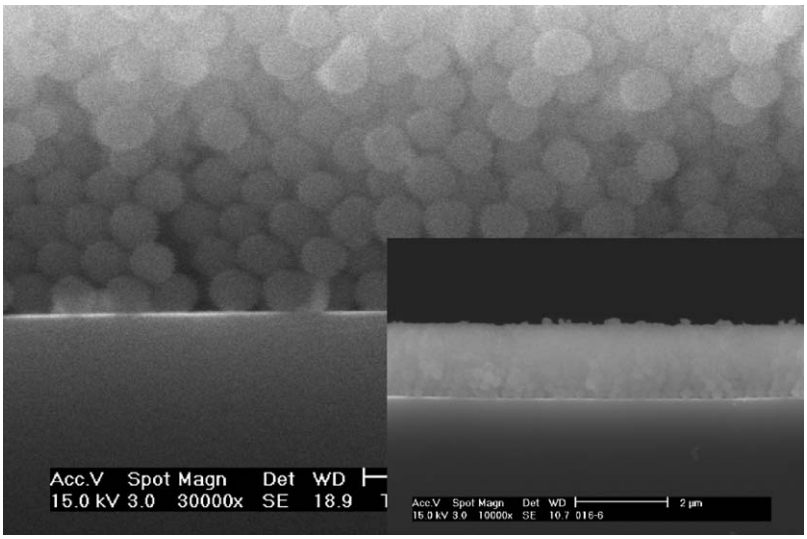

Fig. 3. SEM image of a cleaved edges of the sample infiltrated opal of magnifying 30 000 doubles. The inset is the same sample of magnifying 10 000 doubles.

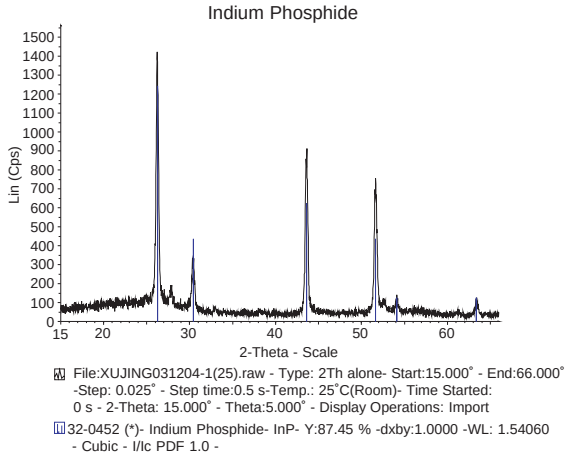

Fig. 4. XRD spectra of InP–SiO_2 photonic crystals.

incidence angle (perpendicular to the surface) for bare and InP infilled opals made up to 250 nm spheres (10 layers). In Fig. 5, we observed the Bragg reflection peaks coming from the coherent scattering of light caused by the crystalline planes of submicrometric opal spheres. One can notice that the maximum peak of the bare opal is at 502 nm. However, the InP infilled opal is 540 nm. Thus, we can conclude that the infilling with high refractive index materials provokes a shift of the Bragg reflections towards higher wavelengths. The result indicates that the InP is the homogeneous distribution of the voids between opal spheres, which is in agreement with the SEM images. For Bragg reflections arise from the 3D order in the samples and the shift of the (1 1 1) optical band is only possible if a homogeneous distribution of the InP infilled exists.

These optical characterization results can be explained using Bragg law in the air:

$$2d_{(111)}\sin\theta = \lambda, \tag{1}$$

but in the dielectric, the law should be modified by [17]

$$\lambda c = 2d_{(111)}(\varepsilon_{av} - \cos^2\theta)^{1/2}, \tag{2}$$

where $d_{(111)}$ is the distance between crystallines planes in the (1 1 1) direction. In this work, $d_{(111)} = 0.816a$ (a is the diameter of the opal spheres) for the FCC structure, θ is the angle between the incident radiation and the sample (1 1 1) surface ($\theta = 90^\circ$), ε_{av} is the average dielectric constant of the composite, which can be approximated by the expression:

$$\varepsilon_{av} = f\varepsilon_{SiO_2} + f'\varepsilon_{InP} + f''\varepsilon_{air}, \tag{3}$$

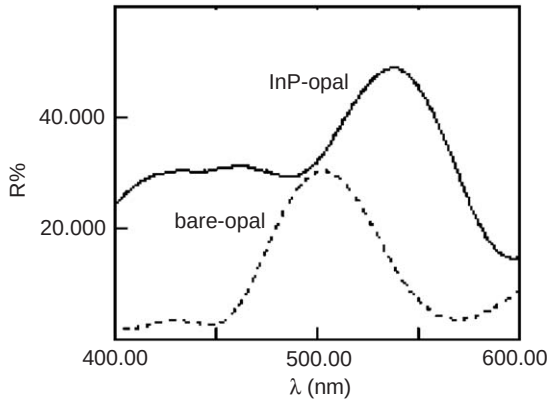

Fig. 5. Specular reflectance for a bare opal (dashed line) and the same opal infiltrated with InP.

where f, f', f'' are the filling ratios of silica ($f = 0.74$), InP and air in the voids, respectively ($f' + f'' = 0.26$). It can be easily seen from expression (2) that InP-infilled samples present higher average dielectric constant. With ε_{av} increasing, λc shifts towards longer wavelengths. So, it can be concluded that infilled samples should present Bragg reflections at higher wavelengths when compared with those coming from bare ones. Experimental results shown here are in good agreement with these considerations.

According to Eqs. (1) and (2), the amount of InP can be estimated. We have calculated that the filling ratios of InP in the voids is about 12.8%.

In Fig. 5, we noticed that the intensity coming from the opals-infiltrated InP is larger than that of bare opals. The enhancement of the photonic crystal properties in InP infilled samples is due to the consideration that a low ε matrix causes a large increase in the scattering strength ε_r of the periodic composite. Since InP has a very high dielectric constant ($\varepsilon \approx 12.7$), even low InP loads yields a substantial increase of ε_{av}.

Accordingly, optical experiments are in good agreement with the theoretical considerations indicated above. The change in the optical behavior observed indicates that the infilled material is 3D homogeneously distributed in the host.

4. Conclusions

In this paper, a technique in which the opal was infiltrated with InP by LP-MOCVD is introduced, aiming at the fabrication of large-area high-performance InP photonic crystal. The InP was proved to be of high quality by SEM and reflectance spectroscopy. The photonic crystal properties of the samples is enhanced with the InP infiltrated.

Acknowledgements

This work was supported by the National Advanced Materials Committee of China and the National Nature Science Foundation of China.

References

[1] E. Yablonovitch, Phys. Rev. Lett. 89 (1987) 2059.
[2] V.N. Bogomolov, S.V. Gaponenko, A.M. Kapitonov, A.V. Prokofiev, A.N. Ponyavina, N.I. Silvanovich, S.M. Samoilovich, Appl. Phys. A 63 (1996) 613.
[3] Yu.A. Vlasov, V.N. Astratov, O.Z. Karimov, A.A. Kaplyanskii, V.N. Bogomolov, A.V. Prokofiev, Phys. Rev. B 55 (1997) R13357.
[4] V.N. Bogomolov, S.N. Gaponenko, L.N. Germanenko, A.M. Kapitonov, E.P. Petrov, N.V. Gaponenko, A.V. Prokofiev, A.N. Ponyavina, N.I. Silvanovich, S.M. Samoilovich, Phys. Rev. E 55 (1997) 7619.
[5] H. Migues, C. Lopez, F. Meseguer, A. Blanco, L. Vazquez, R. Mayoral, M. Ocana, V. Fornes, A. Mifsud, Appl. Phys. Lett. 71 (1997) 1148.
[6] A.V. Barysev, A.A. Kaplyanskii, V.A. Kosobuki, M.F. Limonov, K.B. Samusev, D.E. Usvyat, Physica E 17 (2003) 426.
[7] N.P. Johnson, D.W. McComb, A. Richel, B.M. Treble, R.M. De La Rue, Synth. Met. 116 (2001) 469.
[8] A.L. Reynolds, D. Cassagne, C. Jouanin, J.M. Arnold, Synth. Met. 116 (2001) 453.
[9] B.Y. Cheng, P.G. Ni, Ch.J. Jin, Zh.L. Li, D.Zh. Zhang, P. Dong, X.C. Guo, Opt. Commun. 170 (1999) 41.
[10] S.G. Romanov, N.P. Johnson, A.V. Fokin, V.Y. Butko, H.M. Yates, M.E. Pemble, C.M. Sotomayor Torres, Appl. Phys. Lett. 70 (1997) 2091.
[11] Yu.A. Vlasov, K. Luterova, I. Pelant, B. Honerlage, V.N. Astratov, Appl. Phys. Lett. 71 (1997) 1616.
[12] H.M. Yates, M.E. Pemble, N.J. Johnson, S.G. Romanov, C.M. Sotomayor Torres, J. Crystal Growth 170 (1997) 611.
[13] O. Vickreva, O. Kalinina, E. Kumacheva, Adv. Mater. 12 (2000) 110.

[14] M.I. Samoilovich, S.M. Samoilovich, A.V. Guryanov, M.Y. Tsvetkov, Microelectron. Eng. 6 69 (2003) 237.
[15] C. Lopez, L. Vazquez, F. Meseguer, R. Mayoral, M. Ocana, Superlattices Microstruct. 22 (1997) 399.
[16] M. Trau, D.A. Saville, I.A. Aksay, Langmuir 13 (1997) 6375.
[17] H.M. Yates, M.E. Pemble, H. Miguez, A. Blanco, C. Lopez, F. Meseguer, L. Vazquez, J. Crystal Growth 193 (1998) 9.